

# Discovery of Red Selected Arcs at $z=4.04$ behind Abell 2390

Brenda Frye and Tom Broadhurst

Department of Astronomy, University of California, Berkeley, CA 94720

## ABSTRACT

We describe the properties of a system of red arcs discovered at  $z=4.04$  around the cluster A2390 ( $z = 0.23$ ). These arcs are images of a single galaxy, where the lensing is compounded by an elliptical cluster member lying close to the critical curve of the cluster. The combined magnification is estimated to be  $\sim 20$ , using HST images, depending the gradient of the model potentials, implying an unlensed magnitude for the source of  $I_{AB} = 25.5$ . Keck spectroscopy reveals a continuum well fitted by B-stars and attenuated by the Lyman-series forest with an opacity consistent with  $z\sim 4$  QSO spectra, making the arcs relatively red. Damped Ly $\alpha$  absorption is observed at the source redshift with a relatively high column,  $n_{HI} = 3 \times 10^{21}$ . Curiously, Ly $\alpha$  emission is spatially separated ( $\sim 0.5$ kpc) from the bright stellar continuum and lies  $\sim 300$ Km/s redward of interstellar absorption lines at  $z=4.04$ . Similar redward shifts are found in all high redshift galaxies with good spectroscopy, indicating that outward flows of enriched gas are typical of young galaxies. Finally, we briefly comment on the notorious “straight arc” in A2390, which is resolved into two unrelated galaxies at  $z=0.913$  and  $z=1.033$ .

*Subject headings:* cosmology: gravitational lensing — cosmology: observations — galaxies: clusters: individual (Abell 2390) — galaxies: distances and redshifts

## 1. Introduction

Magnification by galaxy clusters is responsible for the discovery of many distant galaxies. A clear example is the mirror symmetric arc straddling the critical curve of A2218 (Kneib *et al.* 1996) which is found to lie at  $z = 2.51$  (Ebbels *et al.* 1996). A much brighter object “CB58” with  $V = 20$  and  $z = 2.72$ , was discovered in a redshift survey of the cluster MS1512+36 (Yee *et al.* 1996). This object does not form an obvious arc but appears to be an example of a fold image of an intrinsically small source (Seitz *et al.* 1996) and hence near maximally magnified for its size, so that it lies obliquely across the critical curve. More

distant galaxies were uncovered by Trager *et al.* 1997, at redshifts 3.34 and 3.98, behind the core of a more distant cluster A851,  $z = 0.41$ , (Dressler and Gunn 1992), in a study of irregular cluster members. A flat central potential is the most reasonable explanation here, generating similar tangential and radial stretching, so the effect of lensing is mainly an enlargement of images with little change in shape, not inconsistent with the weak distortions claimed in the field of this cluster (Seitz *et al.* 1996). For intermediate redshift clusters like this, the magnification of distant galaxies is maximal for a flat potential. Most analogous to the lensed galaxy presented here are the red arcs discovered by Franx *et al.* (1997) at  $z = 4.92$ , behind the cluster CL1358+62 ( $z = 0.33$ ). Here the magnification of the main arc is compounded by the potentials of the cluster and an elliptical member.

In this letter we describe a lensed system of arcs at  $z = 4.04$ , discovered behind the massive lensing cluster A2390 ( $z = .231$ ) in a redshift survey of faint red objects behind massive clusters. We demonstrate that these arcs are all images of one highly magnified galaxy and that their spectra are attenuated by the the expected level of foreground Lyman-forest absorption. We find evidence for gas outflow in common with both other high redshift galaxies and well studied local starburst galaxies. This object is the first very distant galaxy discovered in our general survey of red cluster background objects.

## 2. Observations

HST images of A2390 were used to select galaxies redder than the cluster sequence for spectroscopy with the Keck. The imaging observations (courtesy of B. Fort) comprise four long exposures totaling 160 minutes in each of the F555W and F814W bands, corresponding roughly to V and I. These images were aligned to the nearest integer and then cosmic rays rejected separately in each passband. Figure 1 (see Plate) shows a color representation of the center of cluster. A striking lensing pattern is visible, including the famous straight arc (Mellier 1989, Pelló *et al.* 1991). A very bright and dusty red object is also seen lying along the critical curve ( $z = 0.81$ ), as well as several lensed background elliptical galaxies which are redder than the cluster E/SO's due simply to their larger k-corrections (Frye *et al.* 1998). The multiply lensed high redshift images reported here are visible as relatively red and thin arcs with similar substructure along their lengths, centered on a bright cluster elliptical. Removal of this elliptical by ellipse subtraction reveals 4 similar images forming a stretched set of four arcs, as indicated in Figure 1b.

Targets for multislit spectroscopy were then selected from the HST field and supplemented by others registered on larger CFHT images, in a general redshift survey of lensed red galaxies selected with  $V-I > 1.5$  and  $I < 24$ . Instrument flexure, fringing and

the large quantity of spectroscopy requires a purpose built code for efficient and accurate reduction. Details of the data reduction and the redshift survey are presented by Frye *et al.* (1998), complimenting the brighter limited survey of the main arcs by Bezecourt & Soucail (1997). The spectra of the larger arcs, labeled N and S in Figure 1, were taken normal to the long axes of the two bright arcs using the W. M. Keck I telescope in August 1996 in one hour of exposure, using LRIS with the 300 line grating and a slit width of  $1.5''$ , resulting in a resolution of  $15.6 \text{ \AA}$  and dispersion of  $2.4 \text{ \AA}$  per pixel. These spectra are flux calibrated and shown in Figures 2a and 2b. The slit width is narrower than the length of these arcs,  $5''$  and  $3''$ , and oriented near perpendicular to their long axes, hence the spectra are not expected to correspond to same spatial section of the source, and their spatial locations are indicated in Figure 1c. Subsequent spectroscopy in August 1997, using the same instrumental configuration (using Keck II) but with slits aligned along the arcs, totaling 2.8hrs of exposure, confirms the high redshift of these arcs through the presence of metal absorption lines. In addition,  $\text{Ly}\alpha$  emission is seen at the Northern end of the Northern arc. A third arc labeled E in Figure 1 was also observed to investigate the lens geometry and found to share the same redshift as the two bright arcs, its spectrum is shown in Figure 2c. The fourth image, W, is too faint for useful spectroscopy.

### 3. Spectral Analysis

Using the flux calibrated spectra of the N and S arcs we find that their continua are very well fitted by a model B3 star (Kurucz 1993), modified by the opacity expected from the Lyman-forest based on QSO spectra, shortward of  $\text{Ly}\alpha$  (as parameterized by Madau 1995), as shown in Figure 2a,b. The lack of O-stars makes this object unusual in comparison to the spectra of other high redshift galaxies. Taken at face value this might simply imply that we are not catching this galaxy in the throws of star-formation but shortly after, at  $10^6 < t < 3 \times 10^7 \text{ yrs}$ , when the O-stars have disappeared. But dust reddening of an O-star population could also be invoked to explain the continuum slope. The lack of flux shortward of restframe  $1000\text{\AA}$  is consistent with the expected fall off of the B-starlight following the Wein tail. However, since this fall off lies close to the Ly-limit at  $912\text{\AA}$ , and better data is needed to discriminate between reddened O-starlight as the source of the continuum emission and unreddened B-stars. Of course the presence of  $\text{Ly}\alpha$  emission requires a source of FUV photons, but since a few O-stars generate a large equivalent-width of emission, then a B-star dominated spectrum is not problematic.

A combined spectrum of the N and S arcs is also shown in figure 2c (unfluxed), from data obtained with slits aligned along the major axes of the arcs. This leads to an accurate

redshift based on metal absorption lines, SII 1260Å, OI 1302Å, SiII 1304Å, CII 1336Å, SiIV 1394Å, 1403Å, and SiIV 1403Å at  $z = 4.04$ . A foreground absorption line is found covering both the N and S arcs, at  $\lambda = 6454\text{Å}$ , most likely corresponding to MgII 2802Å, at  $z = 1.3$ . The metal lines are clearly offset in wavelength from the centroid of the Ly $\alpha$  emission which lies 300Km/s redward of the metal lines (Figure 2). This redward shift is evident from inspection of all high quality spectra of distant galaxies (Steidel *et al.* 1996a,b, Steidel *et al.* (1997), Trager *et al.* (1997), Franx, *et al.* (1997), Lowenthal *et al.* (1997) and is seen in locally in the UV spectra of starburst galaxies (Lequeux *et al.* 1996, Legrand *et al.* 1997), as pointed out by Franx *et al.* (1997). Lequeux *et al.* (1996) explain this shift as arising from back-scattered Ly $\alpha$  photons from the HI shells around expanding HII regions, so that the Doppler redshift of far-side emission is cleared of foreground absorption within the galaxy.

From the spatially resolved data it is clear that the Ly $\alpha$  emission is confined to the northern ends of both the N and S arcs. The non-appearance of Ly $\alpha$  emission in the spectrum of the Northern arc, Figure 2a, is explained by comparison with parallel slit data, which showed our original slit location fell to the south of the Ly $\alpha$  emission (Figure 1b). At this location damped HI absorption is found with a column  $\sim 3 \times 10^{21} n_{HI}$ , sufficient to dilutely spread any resonantly scattered Ly $\alpha$  emission over an undetectably large wavelength range. The damped absorption is much wider than for B-stars, hence such stars do not contribute to the determination of the saturated HI column. The presence of damped absorption would seem to strengthen the relation advocated by Wolfe (1988), between galaxies and high-redshift damped absorbers in general.

#### 4. Lens Model

It is relatively straightforward to reproduce the basic properties of the lensed image configuration. For generating four images stretched along the major axis of the central elliptical member requires a significant deflection from the cluster potential, so that the elliptical member galaxy must lie close to the critical curve of the cluster for a source at  $z = 4$ . Figure 1c shows a reasonable model of the data, where the deflection field is calculated numerically. The critical curve of the cluster joins with that of the elliptical galaxy at 30" from the cluster center. The absolute image separation is set mainly by the cluster mass, and the relative separations of the N-S over the E-W images pairs constrains the ratio of elliptical/cluster masses to be  $\sim 0.03$ , depending somewhat on the ellipticity of the cluster. We fix the ellipticity of the elliptical galaxy to equal that of its light profile,  $b/a = 0.7$ , resulting in a relatively large ellipticity,  $b/a = 0.5$ , for the cluster mass so that the

largest arc, N, can lie closer to the central elliptical than arc S. In addition, an offset of  $\sim 30$  degrees is needed between the major axis of the cluster east of a line connecting the cluster center through the elliptical member. This asymmetry also helps somewhat to reproduce the straightness of the N and S arcs. For fixed ellipticities, the relative image intensities are most sensitive to the gradient of the cluster mass profile, preferring a shallower than isothermal projected slope,  $\theta^{-0.8}$ , at the critical radius, helping to generate a fairly lengthy arc E as observed.

This result is shown in Figure 2 and displays the parity of the images for a simple circular source, where the lighter and darker regions of the arcs are adjusted to correspond to the regions of the observed Ly $\alpha$  emission and the stellar continuum respectively, matching the parallel slit spectroscopy. Also shown is the magnification field, revealing the critical curve, demonstrating the asymmetry required of the mass distribution. The source magnification in this model is  $\sim 20$ . Taking the Northern arc alone and subtracting its magnification from the observed magnitude  $I_{AB} = 23.0$ , yields  $I_{AB} \sim 25.5$  for the intrinsic apparent magnitude, where the largest uncertainty is the slope of the mass profile - the flatter the profile the larger the magnification. The observed magnitudes of the other arcs labeled S,E,W are  $I_{AB}=23.6,24.5,26$ , respectively. The angular diameter of the source in this model is  $\sim 0.2''$ , or between 0.7kpc/h, ( $\Omega=1$ ) and 1.4kpc/h ( $\Omega=0$ ), assuming the source is roughly symmetric. This width is consistent with the poorly width of the in arcs in the HST images (Figure 1b).

Our simple lens model is similar but not as extreme as those explored in the analysis of the notorious straight arc in this cluster, which has proven difficult to reproduce (Kassiola, *et al.* 1992). Interestingly this arc lies very close to our high redshift system, shown in Figure 1, and is well resolved in HST images (see Figure 1b where the adjacent elliptical is removed). This difficulty is alleviated somewhat by the results of our spectroscopy, which show unambiguously that component A (in the notation of Pelló *et al.* 1991) lies at higher redshift,  $z = 1.033$ , than component C, which we confirm to be at  $z = 0.913$ , and indicated in Figure 1b. Hence in our lens modeling we do not invoke an additional dark mass (Kassiola *et al.* 1992) but instead prefer a large ellipticity for the cluster mass distribution. Having said that, it seems clear that this model does not produce the alignment of the nearby N and S arcs, indicating the need for additional tangential shear.

## 5. Discussion and Conclusions

The inferred small size of our distant galaxy fits into the general picture now emerging of galaxy formation by a piecemeal growth of sub-galactic sized objects. The deepest

images of the sky display a surprisingly high surface density of tiny galaxies (Williams *et al.* 1996) and may be interpreted in a model-independent way as evidence for growth on small scales at least (Bouwens, Broadhurst & Silk, 1997, BBS). Little is known about the process by which galaxies emerge from the neutral epoch although clearly the bulk of this transition takes place before  $z \sim 1$ , below which the density of  $L > L^*$  galaxies varies little (Lilly *et al.* 1995, Ellis *et al.* 1996). The Steidel population of Ly-limit selected galaxies found in the range  $2.5 < z < 3.5$  (Steidel *et al.* 1996a, 1996b, Lowenthal, *et al.* 1997) have compact sizes and display far more sub-structure than expected of redshifted spiral galaxies (Bouwens *et al.* 1997). Individual star-formation rates are uncertain, but several 10's of solar masses per year have been inferred for the brightest cases (Pettini *et al.* 1997). Their evolution and relation to low-redshift galaxies is still unclear. By integrating their UV luminosities, Madau *et al.* (1996) infer a steep decline in the integrated rate of star-formation for  $z > 2$ , relying on little evolution in the shape of luminosity function. This steep decline is unnatural in hierarchical models without strong 'feedback' (Cole *et al.* 1994). A simpler explanation for the behaviour of this integral, in the context of a hierarchical scheme, results from the continuous decrease in mean galaxy size and hence luminosity expected with increasing redshift, naturally resulting in fewer galaxies detected above the limiting luminosity. Indeed, flat or *increasing* mean star-formation rates at  $z > 2$  may be accommodated by the the observed dropout populations (Bouwens & Broadhurst 1997) in the range  $2 < z < 6$ .

Lensing by clusters, we have learned, provides a means to access the highest redshift galaxies, aided by fortuitously large magnifications. Fluxes enhanced by magnification effectively increase the magnitude limit, allowing us to sample to higher  $z$  behind the cluster than in the field to a fixed flux limit. However it should be noted that the utility of lensing is compromised by the very magnification,  $\mu$ , one would take advantage of. The surface density of sources is reduced by the expansion of sky area, at a rate  $1/\mu$ , with each galaxy magnified by  $\Delta m = 2.5 \log \mu$ , so that power-law counts transform via  $N(< m) \propto \mu^{2.5\gamma-1}$ , independent of the details of the mass distribution, generating a net *reduction* for faint galaxies where  $\gamma < 0.4$ . This implies a good estimate of the magnification is important both for determining intrinsic luminosities and for estimating the true surface density of source galaxies.

The lensed galaxy presented here provides interesting information on one of the earliest known optically selected galaxies. The cluster magnification has fortuitously afforded us detailed spectral and spatial information of a very faint and presumably otherwise typical example of a galaxy at  $z=4.0$ . Subsequently we have obtained higher resolution longslit spectra revealing spatial and spectral detail of the Ly $\alpha$  and metal lines along the lengths of the N and S arcs (Frye *et al.* 1998) and also near-IR Keck images useful for exploring

the role of dust and for a good estimate of the luminosity (Bunker *et al.* 1997). The rarity of luminous high redshift galaxies and the requirement of a high magnification for useful spectroscopic follow-up means that such searches will be slow, but well rewarded by detailed information on galaxies at otherwise inaccessibly early times.

## 5.1. Figures

We thank Hy Spinrad, Art Wolfe, Genevieve Soucail, Richard Ellis, and Rosa Pelló and Fred Courbin for useful conversations. We also thank Art Wolfe for his Ly $\alpha$  profile generating code and also Joe Morris and Andrea Somer for help with the HST reductions. TJB acknowledges an ST grant NASA grant XYZ.

## REFERENCES

- Bouwens, Broadhurst & Silk 1997 astro-ph/9710291
- Bouwens & Broadhurst 1997 (in prep)
- Bezecourt, J. & Soucail, G. 1997, A&A, 317, 661
- Bunker, A., Moustakas, L. A., Frye, B. L, Broadhurst T.J., Davis. M, & Spinrad, H. 1998, *The Young Universe, Rome*
- Cole, S., Aragon-Salamanca A, Frenk, C.S., Navaro, J.F., Zepf, S.E., 1994 MNRAS 271,781
- Dressler, A. & Gunn, J. E. 1992, ApJS, 78, 1
- Ellis, R. S., Colless M., Broadhurst T.J., Heyl, J., Glazebrook, K., 1996 MNRAS 280,235
- Ebbels, T. M. D., Le-Borgne, J.-F., Pelló, R., Ellis, R. S., Kneib, J.-P., Smail, I., & Sanahuja, B. 1996, MNRAS, 281, L75
- Franx, M., Illingworth, G.D., Kelson, D., VanDokkum, P.G., Pieter, G., Tran, K., 1997 ApJ, 486, L75
- Frye, B., Spinrad, H., Broadhurst T.J., Bunker A., 1998 *in prep*
- Frye, B., Broadhurst T.J., Guhathakurta R, 1997 *in prep*
- Kassiola, A., Kovner, I. & Blandford, R. D. 1992, ApJ, 396, 10
- Kneib, J.P., Ellis, R.S., Samil, I., Couch, W.J., Sharples, R.M., 1996, ApJ . 471 643
- Kurucz, R. L. 1993, CD-ROM, Cambridge, MA: Smithsonian Astrophysical Observatory, c1993
- Lowenthal, J. D., Koo. D. C., Guzman, R., Gallego, J., Phillips, Faber, S. M., Vogt, N. P., Illingworth, G. D., & Gronwall, C. 1997, ApJ, 481, 673

- Lagrand, F., Kunth, D., Mas-Hesse, J. M., Lequeux, J. 1997 *A&A*, 326, 929
- Lequeux, F., Kunth, D., Mas-Hesse, J. M., Sargent, W. L. W.. 1995 *A&A*, 301, 18L
- Lilly, S. J., Tresse, L., Hammer, F., Crampton, D., Le Fevre, O., 1995 *ApJ* 455, 108
- Madau, P., Ferguson, H. C., Dickinson, M. E., Giavalisco, M., Steidel, C. C., and Fruchter, A. 1996, *MNRAS*, 283, 1388
- Madau, P. 1995, *ApJ*, 441, 18
- Mellier, Y. 1989, in *Clusters of Galaxies*, ed. M. Fitchett (Baltimore: Space Telescope Science Institute)
- Pelló, R., Sanahuja, B., Le Borne, J.-F., Soucail, G., & Mellier, Y. 1991, *ApJ*, 366, 405
- Pettini, M., Steidel, C., Adelberger, K. L., Kellogg, M., Dickinson, M., Giavalisco, M., 1997 *Origins* eds Shull *et al.* (ASP Conference Series)
- Seitz, C, Kneib, J.-P., Schneider, P. & Seitz, S. 1996, *A&A*, 314, 707
- Seitz, S, Saglia, R.-P., Bender, R. Hopp. U. Belloni, P., Ziegler, 1996, astro-ph/9706023
- Steidel, C. C., Giavalisco, M., Pettini, M., Dickinson, M., & Adelberger, K. L. 1996a, *ApJ*, 462, 17
- Steidel, C. C., Giavalisco, M., Dickinson, M., & Adelberger, K. L. 1996b, *AJ*, 112, 352
- Trager, S. C., Faber, S. M., Dressler, A. & Oemler, A. 1997, *ApJ*, 485, 92
- Yee, H. K. C., Ellingson, E., Bechtold, J., Carlberg, R. G. & Cuillandre, J.-C. 1996, *AJ*, 111, 1783
- Williams, R. E. *et al.* 1996 *AJ* 112, 1335
- Wolfe, A. M., 1988 *QSO Absorption Lines: Probing the Early Universe*, ed J. C. Blades, D. A. Turnshek, D. A., & C. A. Norman (Cambridge: Cambridge Univ. Press)

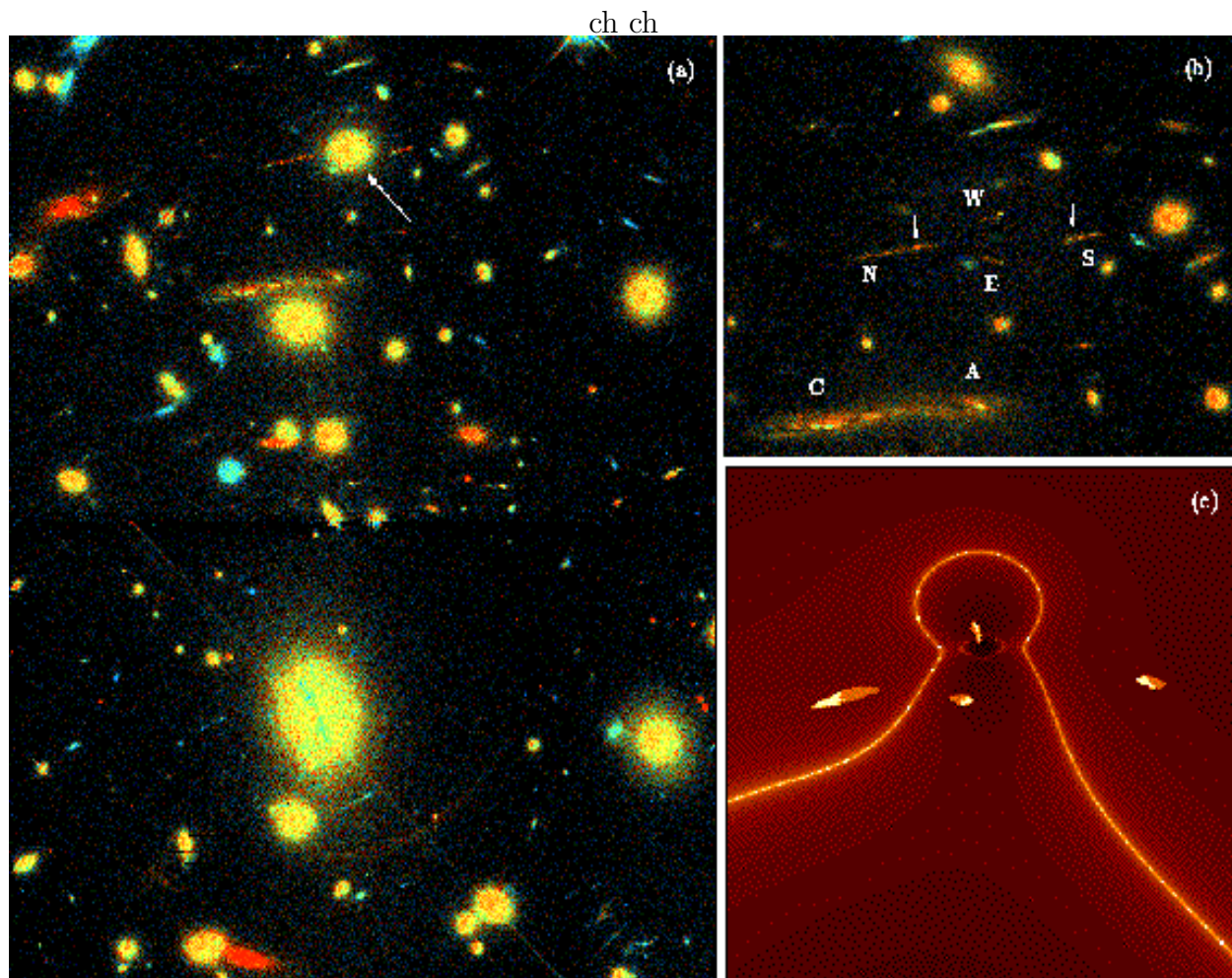
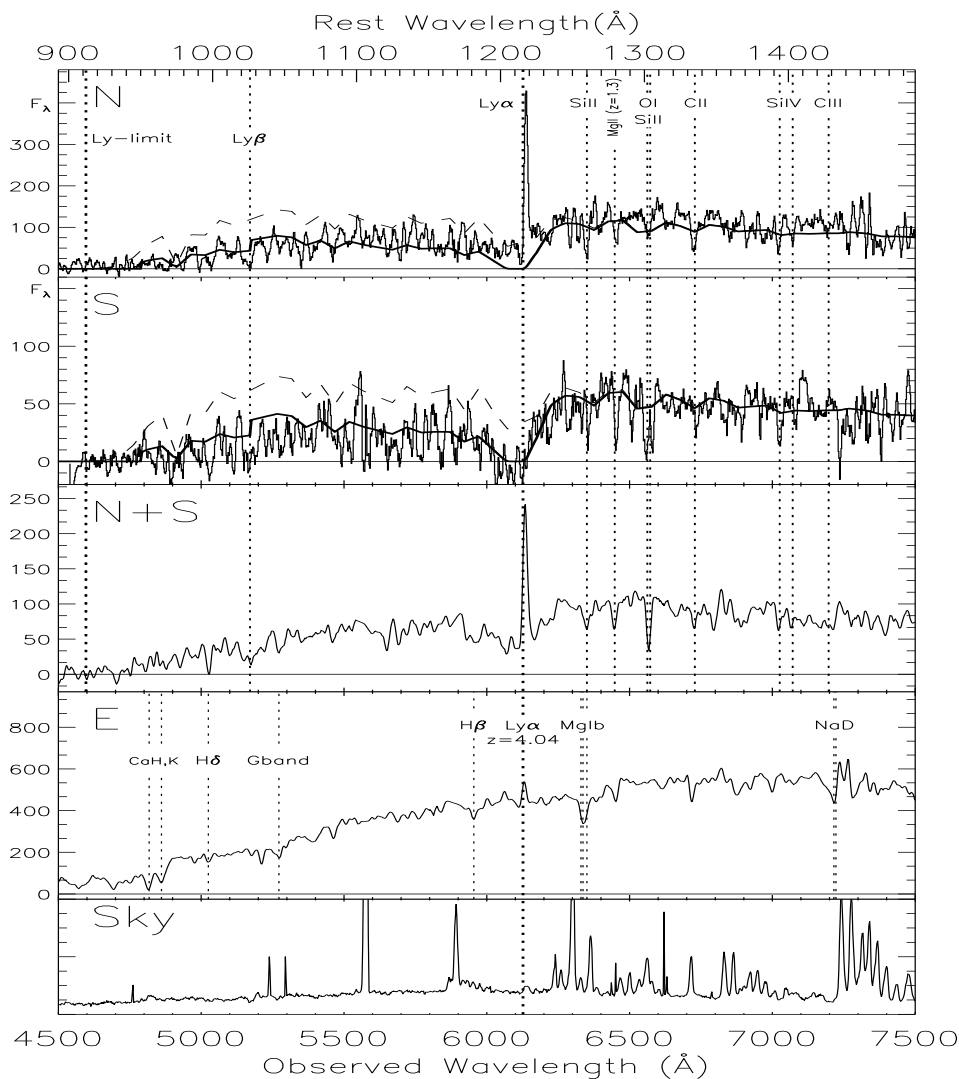


Fig. 1.— Panel (a) shows the many red and blue arcs around the center of A2390, with the elliptical galaxy centered on the  $z=4.04$  arcs indicated. (b) A blow up of the region containing the 4 lensed images of the  $z=4.04$  galaxy, with the central elliptical galaxy removed. The locations of the slitlet positions corresponding to figures 2a,b are indicated. Also shown is the “straight arc” which spectroscopy resolves into two galaxies: component A, at  $z=1.033$  and component C, at the known redshift,  $z=0.913$ . (c) A simple lens model for the source showing the importance of both the central elliptical and the cluster potential in creating the image configuration. The parity of the images is also displayed. The brighter part of the images is chosen to match the spatial location of the observed  $\text{Ly}\alpha$  emission in the N and S arcs. The images are overlaid on the magnification distribution showing clearly the bright asymmetric critical curve.



ch ch

Fig. 2.— **(2)** Keck spectra of the arcs at  $z=4.04$ . The upper two panels show fluxed spectra of the Northern and Southern arcs taken with slits aligned normal to the long axes of these arcs. Overlaid is the best fitting B3-star continuum, with the opacity of the forest included, together with damped  $\text{Ly}\alpha$  absorption at the galaxy redshift, but no reddening. The middle panel shows the sum of both these arcs with slits aligned along their lengths, revealing clearly metal lines at  $z=4.04$ , on which the redshift is based. These lines lie blueward of the centroid of the  $\text{Ly}\alpha$  emission by  $300\text{km/s}$ , as discussed in the text. Below this is shown a spectrum centered on the Eastern arc, revealing  $\text{Ly}\alpha$  emission and the central elliptical ( $z=0.223$ ). The sky is shown for comparison at the bottom of the panel.